Jian-Feng Ma, Chuan-Hao Qu, Yan-Yan Zhou, and Tai-Ping Zhao, 2022, The genesis of ca. 1.78 Ga granitoids in the Xiong'er large igneous province: Implications for continental crust generation: GSA Bulletin, https://doi.org/10.1130/B36694.1.

Supplemental Material

Text. Analysis Method.

Figure S1. Plots of LOI versus major and trace elements for the Gushicun diorites and granites. Lack of correlation between LOI and whole rock major and trace elements indicates that the influence of alteration can be ignored.

TABLE S1. LA-ICP-MS ZIRCON U–Pb ISOTOPIC AND TRACE ELEMENT DATA FOR THE GUSHICUN INTRUSIONS.

TABLE S2. ZIRCON Hf AND O ISOTOPIC DATA FOR THE GUSHICUN INTRUSIONS.

TABLE S3. WHOLE-ROCK MAJOR AND TRACE ELEMENT DATA FOR THE GUSHICUN INTRUSIONS.

TABLE S4. WHOLE-ROCK ND ISOTOPIC DATA FOR THE GUSHICUN INTRUSIONS

SUPPLEMENTAL MATERIAL

The genesis of ~1.78 Ga granitoids in Xiong'er large igneous province: Implications for continental crust generation

Jian-Feng Ma, Chuan-Hao Qu, Yan-Yan Zhou, and Tai-Ping Zhao

ANALYSIS METHOD

Zircon LA-ICP-MS U-Pb dating

Zircon grains were separated using standard magnetic-gravimetric techniques and the selected grains were mounted in epoxy and polished until their cores were exposed. The Gatan MonoCL3 cathode light emitters on a JEOL JXA-8100 Electron Microprobe (EMPA) is used to show the Cathodoluminescence (CL) images of zircon collected. Zircon LA-ICP-MS U-Pb isotopic analyses were conducted independently at the State Key Laboratory of Isotope Geochemistry, Guang zhou Institute of Geochemistry, Chinese Academy of Sciences. U-Pb ages were determined using an Agilent 7500a quadruple (Q)-ICPMS equipped with a GeoLas 200 M ArF excimer 193 nm laserablation system (MicroLas, Germany). A fixed beam diameter of 30μm with a laser repetition rate of 6Hz was adopted. Zircon 91,500 was used as an external calibration standard for age calculation, and NIST610 was analyzed twice for every 10 analyses for concentration calculations of U, Th, and Pb (Günther and Hattendorf, 2005). All analyzed $^{207}Pb/^{206}Pb$, $^{206}Pb/^{238}U$, $^{207}Pb/^{235}U$ and $^{208}Pb/^{232}Th$ ratios were calculated using the Isoplot (ver. 3.00) (Ludwig, 2003).

Lu-Hf isotopic analyses

Zircon Lu-Hf isotopic analyses were performed by using a Nu Plasma II

MC-ICP-MS connected to a RESOLution M-50193 nm laser system. Helium was used as a carrier gas. The spot size was 44 μm, while laser repetition rate was 6 Hz and the energy density applied was 6 J/cm^2. Raw count rates for ^{172}Yb, ^{173}Yb, ^{175}Lu, ^{176}(Hf + Yb + Lu), ^{177}Hf, ^{178}Hf, ^{179}Hf and ^{180}Hf were collected simultaneously. The detail information of analysis strategy and data deduction can be found in published literature (Chu et al., 2002). 91500 and mudtank were reanalyzed as an unknown sample to check the quality of the data during the analysis. The obtained ^{176}Hf/^{177}Hf ratios of the 91500 and mudtank standards were 0.282307 ± 0.000030 (n = 10, 2σ) and 0.282523 ± 0.000024 (n = 10, 2σ), respectively, which are in good agreement with the recommended ^{176}Hf/^{177}Hf ratios within 2σ (0.282311 ± 0.000007, 2σ; 0.282520 ± 0.000016, 2σ) (Wu et al., 2006). The εHf values were calculated using a decay constant for ^{176}Lu of 1.876 × 10^{-11} yr^{-1}(Albarède et al., 2006) and the present-day chondritic ratios of ^{176}Hf/^{177}Hf = 0.282772 and ^{176}Lu/^{177}Hf = 0.0332 (Blichert-Toft and Albarède, 1997).

SIMS zircon oxygen isotope

O isotope analysis were used the Cameca IMS 1280-HR SIMS installed at Guangzhou Institute of Geochemistry, Chinese Academy of Sciences (GIGCAS-SIMS) was employed in this study. Cs^+ primary ions are used to sputtering oxygen ion from zircon samples. The primary beam is ~10 μm in size diameter, and 2-3 nA in intensity. The target area on the sample was pre-sputtered for 35 s using a 20 μm square raster to remove the gold coating. A 10 μm raster was applied during analyses in order to assure a more uniform primary beam and a flat-bottom sputter crater. The contrast

aperture of 400 μm and the field aperture of 5000 × 5000 μm^2 are used. The entrance slit is set at ~125 μm; and the magnification of the transfer system is configured as ~100 (equivalent to an 80 μm). The energy slit was closed to a bandwidth of 50 eV width and shifted 5 eV below the maximum transmission. A normal-incidence electron gun is used to suppress charge. The nuclear magnetic resonance (NMR) controller is used to stabilize the magnetic field. This instrument is operated in the static multi-collector mode with a mass resolution of ~2400 (FWHM) for the multi-collector slit mode is selected 500 μm width slit. The ^{16}O and ^{18}O ions are detected simultaneously by two faraday cups at the L2' and H1 positions, and the currents are amplified by 1010 ohms and 1011 ohms resistors, respectively. The signal intensity of ^{16}O is ~2.0 × 10^9 cps (counts per second) with ~2.2 nA primary beam intensity. A single spot analysis spends 3 min, including the pre-sputtering, centering routines and collecting process, which 2 min is for pre-sputtering and automatic centering in the secondary optics (centering DTFA and DTCA), and 1 min is to integrate 16 cycles of the oxygen isotope signal. The detailed experiment procedure and data reduction strategy are described in Yang et al. 2018.

Whole-rock major and trace element analyses

Samples were crushed and powdered to 200 meshes in an agate mortar. Whole-rock major element analyses were carried out at Guangzhou Institute of Geochemistry (GIG), CAS, using a Rigaku Zsx100e X-ray fluorescence spectrometer on fused glass beads with analytical uncertainty of < 2%. Trace elements were determined with a Bruker M90 inductively coupled plasma mass spectrometry

(ICP-MS) at the Experimental Center of the School of Resources and Environmental Engineering at Hefei University of Technology, Hefei, China, using the method of Qi et al. (2000). Pure elemental standards for external calibration, and OU-1 and AMH-1 as reference materials were used. The accuracies of the ICP-MS analyses are estimated to be better than 5 to 10% (relative) for most elements.

Whole-rock Sm-Nd isotopic analyses

Nd isotope analyses were performed on a Neptune Plus MC-ICP-MS (Thermo Fisher Scientific, Dreieich, Germany) at the Experimental Center of the School of Resources and Environmental Engineering at Hefei University of Technology, Hefei, China. Mass discrimination correction was carried out via internal normalization to a $^{146}Nd/^{144}Nd$ ratio of 0.7219 (Lin et al. 2016). The interference elements Sm have been completely separated by the exchange resin process. The remaining interferences of $^{144}Sm^{+}$ were corrected based on the mothed described by Lin et al. (2016). One JNdi-1 standard was measured every ten samples analyzed. Analyses of the JNdi-1 standard yielded $^{143}Nd/^{144}Nd$ ratio of 0.512118 ± 15 (2SD, n = 31), which is identical within error to their published values (0.512115 ± 07, Tanaka et al., 2000). In addition, the USGS reference materials BCR-2 (basalt) and RGM-2 (rhyolite) yielded results of 0.512644 ± 15 (2SD, n=6) and 0.512810 ± 15 (2SD, n = 4) for $^{143}Nd/^{144}Nd$, respectively, which is identical within error to their published values (Li et al. 2012).

ADDITIONAL REFERENCES

Albarède, F., Scherer, E.E., Blichert-Toft, J., Rosing, M., Simionovici, A., Bizzarro, M., 2006, γ–Ray irradiation in the early Solar System and the conundrum of

the176Ludecay constant: Geochimica et Cosmochimica Acta, v. 70, p. 1261–1270, https://doi.org/10.1016/j.gca.2005.09.027.

Blichert-Toft, J., Albarède, F., 1997, The Lu-Hf isotope geochemistry of chondrites and the evolution of the mantle-crust system: Earth and Planetary Science Letters, v, 148, p. 243–258, https://doi.org/10.1016/S0012-821X(97)00040-X.

Chu, N.C., Taylor, R.N., Chavagnac, V., Nesbitt, R.W., Boella, R.M., Milton, J.A., German, C.R., Bayon, G., Burton, K., 2002, Hf isotope ratio analysis using multi-collector inductively coupled plasma mass spectrometry: an evaluation of isobaric interference corrections: Journal of Analytical Atomic Spectrumetry, v. 17, p. 1567–1574, https://doi.org/10.1039/B206707B.

Günther, D., Hattendorf, B., 2005, Solid sample analysis using laser ablation inductively coupled plasma mass spectrometry: TrAC Trends in Analytical Chemistry, v. 24, p. 255–265, https://doi.org/10.1016/j.trac.2004.11.017.

Li, C.F., Li, X.H., Li, Q.L., Guo, J.H., Li, X.H., Yang, Y.H., 2012, Rapid and precise determination of Sr and Nd isotopic ratios in geological samples from the same filament loading by thermal ionization mass spectrometry employing a single–step separation scheme: Analytica Chimica Acta, v. 727, p. 54–60, https://doi.org/10.1016/j.aca.2012.03.040.

Lin, J., Liu, Y., Yang, Y., Hu, Z., 2016, Calibration and correction of LA–ICP–MS and LA–MC–ICP–MS analyses for element contents and isotopic ratios: Solid Earth Sciences, v. 1, p. 5–27, https://doi.org/10.1016/j.sesci.2016.04.002.

Ludwig, K., 2003, User's manual for ISOPLOT 3.00: a geochronological toolkit for

Microsoft Excel, Special Publication No. 4. Berkeley Geochronology Center 71.

Qi, L., Hu, J., Gregoire, D.C., 2000, Determination of trace elements in granites by inductively coupled plasma–mass spectrometry: Talanta, v. 51, p. 507–513, https://doi.org/10.1016/S0039-9140(99)00318-5.

Tanaka, T., Togashi, S., Kamioka, H., Amakawa, H., Kagami, H., Hamamoto, T., Yuhara, M., Orihashi, Y., Yoneda, S., Shimizu, H., Kunimaru, T., Takahashi, K., Yanagi, T., Nakano, T., Fujimaki, H., Shinjo, R., Asahara, Y., Tanimizu, M., Dragusanu, C., 2000, JNdi-1: a neodymium isotopic reference in consistency with LaJolla neodymium: Chemical Geology, v. 168, p. 279–281, https://doi.org/10.1016/S0009-2541(00)00198-4.

Wu, F.Y., Yang, Y.H., Xie, L.W., Yang, J.H., Xu, P., 2006, Hf isotopic compositions of the standard zircons and baddeleyites used in U–Pb geochronology: Chemical Geology, v, 234, p, 105–126, https://doi.org/10.1016/j.chemgeo.2006.05.003.

Yang, Q., Xia, X., Zhang, W., Zhang, Y., Xiong, B., Xu, Y., Wang, Q., and Wei, G., 2018, An evaluation of precision and accuracy of SIMS oxygen isotope analysis: Solid Earth Sciences, v. 3, no. 3, p. 81-86. https://doi.org/10.1016/j.sesci.2018.05.001.

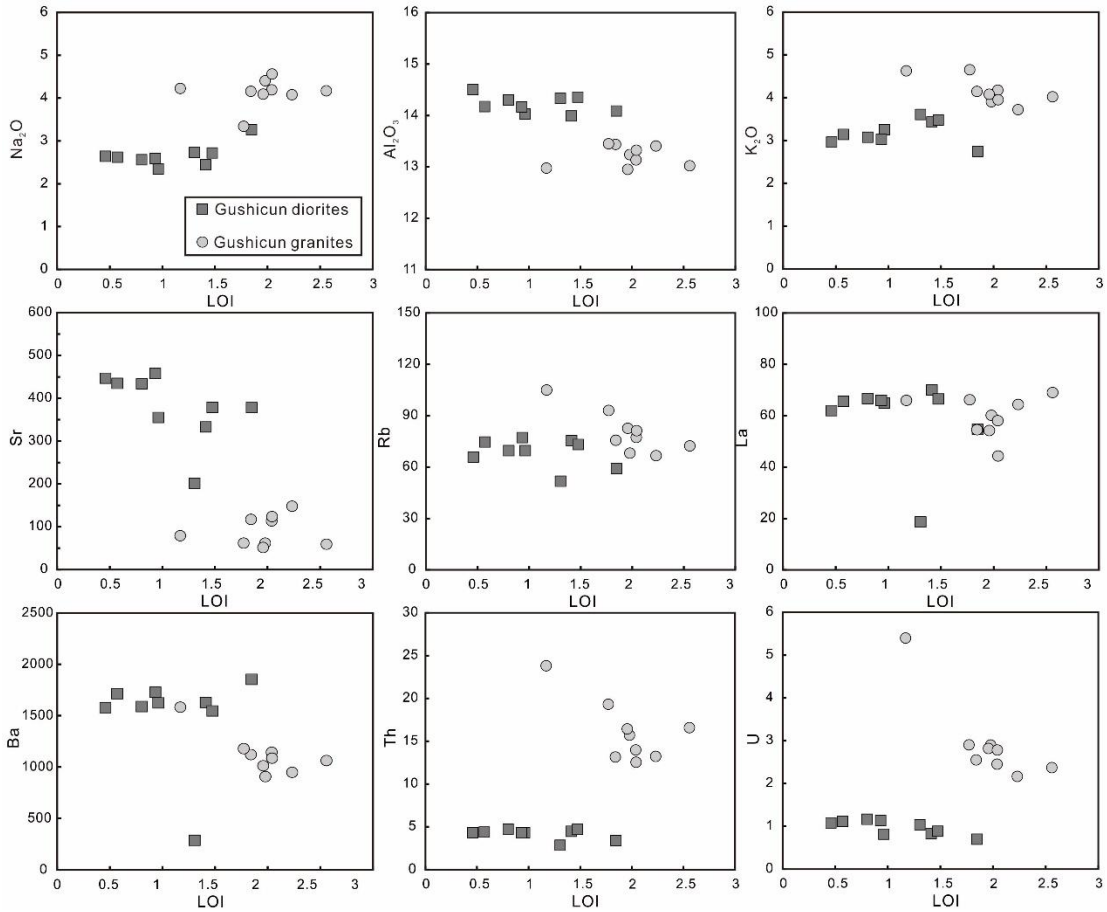

Figure S1. Plots of LOI versus major and trace elements for the Gushicun diorites and granites. Lack of correlation between LOI and whole rock major and trace elements indicates that the influence of alteration can be ignored.